

## Improved power control for an isolated DFIG based WECS

Yasmine IHEDRANE<sup>(1)</sup>, Chakib EL BEKKALI<sup>(1)</sup>, Badre BOSSOUFI<sup>(1,2)</sup>, Madiha EL GHAMRASNI<sup>(3)</sup>, HASSANE MAHMOUDI<sup>(3)</sup>

<sup>(1)</sup>LISTA Laboratory, Faculty of Sciences Dhar El Mahraz. University Sidi Mohammed Ben Abdellah, FEZ, -Morocco-

yasmine.ihedrane@usmba.ac.ma

<sup>(2)</sup>Electrical Engineering and Maintenance Laboratory, Higher School of Technology, Mohammed I University, Oujda-Morocco-

<sup>(3)</sup>Electronic of Power and Control Team (EPCT), Department of Electrical Engineering Mohammadia Engineering School Mohammed V University, Rabat –Morocco-

*Abstract:* - This article, present a new contribution to the control of wind energy systems, a robust nonlinear control of active and reactive power with the use of the Backstepping and Sliding Mode Control approach based on a doubly fed Induction Generator power (DFIG-Generator) in order to reduce the response time of the wind system. In the first step, a control strategy of the MPPT for the extraction of the maximum power of the turbine generator is presented. Subsequently, the Backstepping control technique followed by the sliding mode applied to the wind systems will be presented. These two types of control system rely on the stability of the system using the LYAPUNOV technique. Simulation results show performance in terms of set point tracking, stability and robustness versus wind speed variation.

*Key-Words:* Wind System, DFIG, MPPT, Sliding Mode Controller, Backstepping Controller.

### 1 Introduction

Currently, DFIG-based variable speed wind turbines are most commonly used in wind farms because of its high efficiency, energy quality and the ability to control the power supplied to the grid, as well as the ability to operate in a  $\pm 30\%$  speed range around the synchronous speed, thanks to the design of the three-phase static converters for a portion of the  $\pm 30\%$  nominal power, which makes it possible to reduce the losses in the electronic power components and the overall increase of the system. However, the disadvantage of the DFIG-based wind turbine is that it is very sensitive to load disturbances, turbine rotational speed variation, and variation in internal and external system parameters. Likewise, the double-fed Induction generator is characterized by a nonlinear and multi-variable mathematical model with a strong coupling between the input variables. [1] i.e it is not possible to independently control the voltage or current. For this reason, many implementation works of linear models-based approaches have been applied, but the linear controller approach has quickly shown its limits, that

is why research is oriented towards non-linear techniques to increase the robustness and precision of the systems to be controlled. The main idea of this approach is to analyze the stability of the nonlinear system without solving the differential equations of this system. It is a very powerful tool for testing and finding sufficient conditions for the stability of different dynamic systems.

The study presented in this article aims to optimize the energy performance of a wind turbine to maximize captured wind energy while reducing the problems mentioned above and improving control performance by reducing response time. This optimization is able to minimize the costs of generating electricity. Among these techniques, we find the sliding mode control known for its robustness to changes in external parameters and disturbances, but the disadvantage of this type of control lies in the CHATTERING phenomenon which makes it possible to destabilize the system. The second technique is the non-adaptive BACKSTEPPING control which gives the stability of the nonlinear system, the good tracking ... etc, but which is sensitive to parametric variations[2][3].

In this article, we will carry out a comparative study between the Sliding Mode control techniques and BACKSTEPPING in order to improve the performances of the wind system. We will start by exposing a monetization of the wind turbines. Then, a study of the operating point and maximum power tracking technique will be presented. Subsequently, we present a DFIG model in the "dq" framework and the general principle of controlling both power converters based on the Backstepping and the Sliding Mode control strategy.

## 2 Wind System Modeling

The wind system is mainly composed of the wind turbine, gearbox, the doubly fed induction generator whose stator is directly connected to the grid and the rotor is connected via the Rotor Side Converter (RSC) and the Grid Side Converter (GSC) as shown in the following figure:

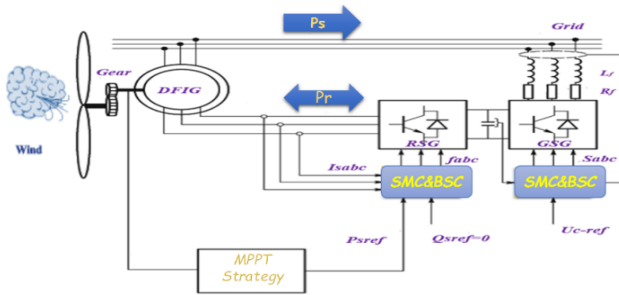


Figure. 1 Global Wind energy conversion system

### 2.1 Wind Turbine Model

The power generated by the wind turbine is modeled from the following equations [7, 8]:

$$P_{aero} = C_p(\lambda, \beta) \cdot \frac{\rho \cdot \pi \cdot R^2 \cdot V^3}{2} \quad (1)$$

Where : R is the turbine radius in m, V is the wind Speed m/s , ρ is the air density in Kg/m<sup>3</sup> and Cp presents the power coefficient which depends on the pitch angle β and the tip speed ratio λ :

$$\lambda = R \cdot \frac{\Omega_t}{v} \quad (2)$$

The expression of the power coefficient is given by the following equation:

$$C_p(\lambda, \beta) = C_1 \left( \frac{C_2}{A} - C_3 \beta - C_4 \right) \cdot \exp \left( -C_5 \cdot \left( \frac{1}{(\lambda + 0.08\beta)} - \frac{0.035}{\beta^3 + 1} \right) \right) + C_6 \lambda \quad (3)$$

Where: C1 =0 .5176, C2 = 116, C3 =0 .4, C4 = 5, C5 = 21, C6 =0 .0068.

The mechanical speed and the mechanical torque that appear on the generator shaft are represented respectively by:

$$\begin{cases} \Omega_t = \frac{\Omega_{mec}}{G} \\ C_g = \frac{C_{aero}}{G} \end{cases} \quad (4)$$

In this work, we fixed the pitch angle and the tip speed ratio to their optimal values λ<sub>opt</sub> =8 and β=0° in order to provide an optimal power from the wind.

### 2.2 Standalone DFIG Model

The Doubly Fed Induction Generator DFIG model using Park transformation is presented by the following equations [6-13] [23-24]:

Stator and rotor voltages in the reference of Park:

$$\begin{cases} V_{sd} = R_s \cdot I_{sd} + \frac{d\phi_{sd}}{dt} - \omega_s \cdot \phi_{sq} \\ V_{sq} = R_s \cdot I_{sq} + \frac{d\phi_{sq}}{dt} + \omega_s \cdot \phi_{sd} \\ V_{rd} = R_r \cdot I_{rd} + \frac{d\phi_{rd}}{dt} - \omega_r \cdot \phi_{rq} \\ V_{rq} = R_r \cdot I_{rq} + \frac{d\phi_{rq}}{dt} + \omega_r \cdot \phi_{rd} \end{cases} \quad (5)$$

Stator and rotor Flux in the reference of Park:

$$\begin{cases} \Phi_{sd} = L_s \cdot I_{sd} + M \cdot I_{rd} \\ \Phi_{sq} = L_s \cdot I_{sq} + M \cdot I_{rq} \\ \Phi_{rd} = L_r \cdot I_{rd} + M \cdot I_{sd} \\ \Phi_{rq} = L_r \cdot I_{rq} + M \cdot I_{sq} \end{cases} \quad (6)$$

Electromagnetic Torque:

$$C_{em} = p \cdot (\Phi_{sd} \cdot I_{sq} - \Phi_{sq} \cdot I_{sd}) \quad (7)$$

Active and reactive DFIG powers:

$$\begin{cases} P_s = V_{sd} \cdot I_{sd} + V_{sq} \cdot I_{sq} \\ Q_s = V_{sq} \cdot I_{sd} - V_{sd} \cdot I_{sq} \end{cases} \quad (8)$$

### 2.3 Converter Model

Voltages across a, b, c rotor windings of the DFIG are constructed using the rotor side converter as follows [3]:

$$\begin{bmatrix} V_{an} \\ V_{bn} \\ V_{cn} \end{bmatrix} = \frac{V_{dc}}{3} \begin{bmatrix} 2 & -1 & -1 \\ -1 & 2 & -1 \\ -1 & -1 & 2 \end{bmatrix} \begin{bmatrix} f_1 \\ f_2 \\ f_3 \end{bmatrix} \quad (9)$$

Where f1, f2 and f3 present the control signals and Vdc is the DC-link voltage as given in [4].

### 2.4 Filter (R,L) Model

The GSC Converter is connected to the DC-BUS and the Grid via a filter (Rf, Lf). It has two roles: sustaining the DC- BUS voltage constance regarding the amplitude and the rotor power direction and maintaining a unit power factor at the link point to the grid [14].The filter model in the referential (d, q) is given by equation (10):

$$\begin{cases} v_{df} = -R_f I_{df} - L_f \frac{dI_{df}}{dt} + \omega_s L_f I_{qf} + v_{sd} \\ v_{qf} = -R_f I_{qf} - L_f \frac{dI_{qf}}{dt} - \omega_s L_f I_{df} + v_{sq} \\ P_f = v_{df} I_{df} + v_{qf} I_{qf} \\ Q_f = v_{qf} I_{df} - v_{df} I_{qf} \end{cases} \quad (10)$$

### 3 Maximum power extraction using MPPT

In order to extract the maximum power from the wind, we need an algorithm acting on the set point variables to have a good efficiency of the device. For this reason, we applied a technique of Maximum Power Point Tracking Strategy. This latter consists in imposing a torque of reference so as to permit the DFIG to turn at a regulating speed to ensure an optimal operating point of power extraction. That is why the speed ratio  $\lambda$  must keep its optimum value ( $\lambda = \lambda_{opt}$ ) over a certain range of wind speed. Furthermore, the power coefficient would be maintained at its maximum value ( $C_{pmax} = C_p$ ) [4]. In this case, the aerodynamic couple will have as an expression:

$$C_{aero} = C_{p\_max}(\lambda, \beta) \cdot \frac{\rho \cdot \pi \cdot R^2 \cdot V^3}{2 \cdot \Omega_t} \quad (11)$$

The reference torque at the output of the multiplier becomes:

$$C_{g\_ref} = \frac{1}{G} \cdot C_{aero} \quad (12)$$

We know that the fundamental equation of dynamics is given by:

$$C_{mec} = J \frac{d\Omega_{mec}}{dt} = C_g - C_{em} - C_f \quad (13)$$

We assumed that the generator rotational speed is fixed during the study period, and we neglected the effect of the viscous torque. The reference electromagnetic torque can be expressed by:

$$C_{emref} = C_g \quad (14)$$

The estimated wind speed can be written as suggested:

$$V_{est} = R \cdot \frac{\Omega_{t\_est}}{\lambda_{est}} \quad (15)$$

The expression of the reference electromagnetic torque can be written as indicated:

$$C_{emref} = \frac{C_{p\_max}}{\lambda_{opt}^3} \cdot \frac{\rho \cdot \pi \cdot R^5}{2} \cdot \frac{\Omega_{mec}^2}{G^3} \quad (16)$$

Based on these equations, we can create the following diagram of the mechanical part of the wind system and the MPPT strategy without speed measurement shown in Fig.3 [4, 6]:

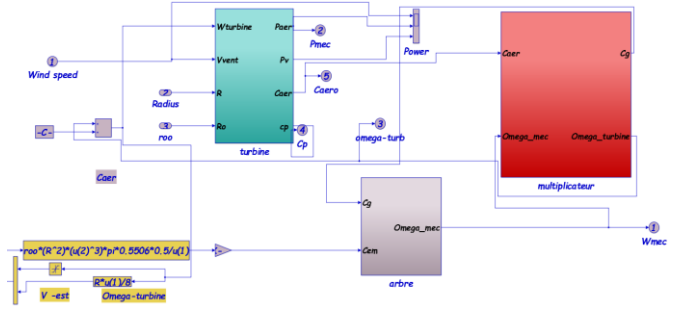


Figure.2: the MPPT strategy without speed measurement

### 4 Non-Linear Controllers Synthesis

The main objective of the DFIG-based WECS control is to maintain a constant stator voltage amplitude and frequency when the wind speed is changed. For this reason, the presence of a controller is very necessary. Many control techniques are developed in the literature for such systems. However, the implementation of these controllers seems very complicated. In this work, two non-linear controllers are developed:

- SLIDING MODE controller
- BACKSTEPPING controller

#### 4.1 Sliding Mode Controller Design

The variable structure system (VSS) is a system whose structure changes during its operation. It is characterized by the choice of a structure and a switching logic. This latter allows the system to switch from one structure to another at any time by the choice of a function, which separates the state space into two parts, and an appropriate switching logic. The Sliding mode technique is a special case of (VSS). It consists of forcing the system state trajectory to attain a hyper surface in finite time and then stay there. This latter presents a relation between the system state variables which defines a differential equation, and consequently, determines the system dynamics if it remains on the hyper surface. The evolution of a system subject to a control law no longer depends on the system or the external disturbances, but on the properties of the hyper surface. The system will therefore be robust to uncertainties (specific to the system) and disturbances (external to the system) but will be totally insensitive [5, 15, 16].

#### 4.1.1 RSC control using Sliding Mode Controller

The sliding surface proposed by J.SLOTINE is given by [17]:

$$s(X) = \left( \frac{d}{dt} + \delta \right)^{n-1} e(X) \quad (17)$$

We take  $n=1$ , we obtain:

$$\begin{cases} S(P_s) = P_{sref} - P_s \\ S(Q_s) = Q_{sref} - Q_s \end{cases} \quad (18)$$

With:  $Q_{sref}$  and  $P_{sref}$  are the reactive and active powers references.

The derivative of sliding surface is given by:

$$\begin{cases} \dot{S}(P_s) = \dot{P}_{sref} + \frac{V_s \cdot M}{L_s} \left( \frac{V_{rqeq} + V_{rqn}}{L_r \cdot \sigma} - \frac{R_r}{L_r \cdot \sigma} \cdot I_{rq} - \omega_r \cdot I_{rd} - \omega_r \cdot V_s \cdot \frac{M}{L_r \cdot L_s \cdot \omega_s \cdot \sigma} \right) \\ \dot{S}(Q_s) = \dot{Q}_{sref} + V_s \cdot \frac{M}{L_s} \left( \frac{V_{rdq} + V_{rdn}}{L_r \cdot \sigma} - \frac{R_r}{L_r \cdot \sigma} \cdot I_{rd} + \omega_r \cdot I_{rq} \right) \end{cases} \quad (19)$$

During the sliding and permanent mode, we have:

$$S(P_s, Q_s) = 0, \dot{S}(P_s, Q_s) = 0, V_{rdn} = V_{rqn} = 0 \quad (20)$$

The expression of the equivalent command becomes:

$$\begin{cases} V_{rdeq} = -\frac{L_r \cdot L_s \cdot \sigma}{M \cdot V_s} \cdot \dot{Q}_{sref} + R_r \cdot I_{rd} - \omega_r \cdot L_r \cdot \sigma \cdot I_{rq} \\ V_{rqeq} = -L_r \cdot L_s \cdot \frac{\sigma}{V_s \cdot M} \cdot \dot{P}_{sref} + R_r \cdot I_{rq} + L_r \cdot \omega_r \cdot \sigma \cdot I_{rd} + \omega_r \cdot M \cdot \frac{V_s}{L_s \cdot \omega_s} \end{cases} \quad (21)$$

Therefore, the stabilizing control is given by the following equation:

$$\begin{cases} V_{rdn} = K_{d sat}(S(P_s)) \\ V_{rqn} = K_{q sat}(S(Q_s)) \end{cases} \quad (22)$$

#### 4.1.2 GSC control using Sliding Mode controllers

We consider the SLOTINE's sliding mode surface. For  $n = 1$ , we obtain:

$$\begin{cases} S(P_f) = P_{fref} - P_f \\ S(Q_f) = Q_{fref} - Q_f \end{cases} \quad (23)$$

Where:  $Q_{fref}$  and  $P_{fref}$  are the reactive and active powers references.

The derivative of the sliding surface is given by:

$$\begin{cases} \dot{S}(P_f) = \dot{P}_{fref} + \frac{V_s \cdot R_f}{L_f} \cdot I_{qf} + \frac{V_s (V_{qfeq} + V_{qfn})}{L_f} + w_s \cdot V_s \cdot I_{df} - \frac{V_s^2}{L_f} \\ \dot{S}(Q_f) = \dot{Q}_{fref} - \frac{V_s \cdot R_f}{L_f} \cdot I_{df} - \frac{V_s (V_{dfeq} + V_{dfn})}{L_f} + w_s \cdot V_s \cdot I_{qf} \end{cases} \quad (24)$$

In the sliding and permanent mode, we obtain the expression of the equivalent command supplied as follows:

$$\begin{cases} V_{dfeq} = \frac{L_f}{V_s} \cdot \dot{Q}_{fref} - R_f \cdot I_{df} + L_f \cdot w_s \cdot I_{qf} \\ V_{qfeq} = -\frac{L_f}{V_s} \cdot \dot{P}_{fref} - R_f \cdot I_{qf} - L_f \cdot w_s \cdot I_{df} + V_s \end{cases} \quad (25)$$

The stabilizing control is expressed by:

$$\begin{cases} V_{dfn} = K_{dfn sat}(S(P_f)) \\ V_{qfn} = K_{qfn sat}(S(Q_f)) \end{cases} \quad (26)$$

## 4.2 Backstepping Controller Design

The principle of Backstepping control is based on the decomposition of the entire control system, which is generally multivariable and of high order into a cascade of first-order control subsystems. For each subsystem, a so-called virtual control law is calculated. The latter will serve as a reference for the next subsystem until obtaining the control law for the complete system. Moreover, this technique has the advantage of preserving the non linearities useful for the performance and the robustness of the control, unlike the linearization methods. The determination of control laws that follows from this approach is based on the use of control Lyapunov functions [9] [20, 21].

### 4.2.1 RSC control using Backstepping controllers

The synthesis of this control can be achieved in two steps [10]:

#### Step 1: Calculation of reference rotor currents:

In this step, we define the error between the active and reactive stator powers and their references. The errors of the stator power are defined by:

$$\begin{cases} e_1 = P_{sref} - P_s \\ e_2 = Q_{sref} - Q_s \end{cases} \quad (27)$$

The derivative of the errors is given by:

$$\begin{cases} \dot{e}_1 = \dot{P}_{sref} - \dot{P}_s \\ \dot{e}_2 = \dot{Q}_{sref} - \dot{Q}_s \end{cases} \quad (28)$$

With:

$$\begin{cases} \dot{P}_s = -\frac{V_s \cdot M}{L_s} \cdot \dot{I}_{rq} \\ \dot{Q}_s = -\frac{V_s \cdot M}{L_s} \cdot \dot{I}_{rd} \end{cases} \quad (29)$$

By replacing each term, by its expression, we obtain the following equation:

$$\begin{cases} \dot{e}_1 = \dot{P}_{sref} + \frac{V_s \cdot M}{L_s} \left( \frac{V_{rq}}{L_r \cdot \sigma} - \frac{R_r}{L_r \cdot \sigma} \cdot I_{rq} - \omega_r \cdot I_{rd} - \omega_r \cdot V_s \cdot \frac{M}{L_r \cdot L_s \cdot \omega_s \cdot \sigma} \right) \\ \dot{e}_2 = \dot{Q}_{sref} + V_s \cdot \frac{M}{L_s} \left( \frac{V_{rd}}{L_r \cdot \sigma} - \frac{R_r}{L_r \cdot \sigma} \cdot I_{rd} + \omega_r \cdot I_{rq} \right) \end{cases} \quad (30)$$

We first choose the candidate function of "LYAPUNOV" associated with the active and reactive stator power errors, in the following quadratic form:

$$V_1 = \frac{1}{2} e_1^2 + \frac{1}{2} e_2^2 \quad (31)$$

Its derivative is given by:

$$\dot{V}_1 = e_1 \dot{e}_1 + e_2 \dot{e}_2 \quad (32)$$

By replacing the error by their expression, we obtain:

$$\begin{aligned} \dot{V}_1 = e_1 \left( \dot{P}_{sref} + \frac{V_s M}{L_s} \left( \frac{V_{rq}}{L_r \sigma} - \frac{R_r}{L_r \sigma} I_{rq} - \omega_r I_{rd} - \omega_r V_s \frac{M}{L_r L_s \omega_s \sigma} \right) \right) + \\ e_2 \left( \dot{Q}_{sref} + V_s \frac{M}{L_s} \left( \frac{V_{rd}}{L_r \sigma} - \frac{R_r}{L_r \sigma} I_{rd} + \omega_r I_{rq} \right) \right) \end{aligned} \quad (33)$$

In order to ensure the stability of the subsystem according to LYAPUNOV,  $\dot{V}_1$  must be negative. So, we choose it in the following form:

$$\dot{V}_1 = -K_1 e_1^2 - K_2 e_2^2 \leq 0 \quad (34)$$

With:  $k_1, k_2$  are positive constants.

Equalizing the two equations, we obtain:

$$\begin{cases} e_1 \left( \dot{P}_{sref} + \frac{V_s M}{L_s} \left( \frac{V_{rq}}{L_r \sigma} - \frac{R_r}{L_r \sigma} I_{rq} - \omega_r I_{rd} - \omega_r V_s \frac{M}{L_r L_s \omega_s \sigma} \right) \right) = -K_1 e_1^2 \\ e_2 \left( \dot{Q}_{sref} + V_s \frac{M}{L_s} \left( \frac{V_{rd}}{L_r \sigma} - \frac{R_r}{L_r \sigma} I_{rd} + \omega_r I_{rq} \right) \right) = -K_2 e_2^2 \end{cases} \quad (35)$$

Which gives the expression of the virtual command  $I_{rd}$  and  $I_{rq}$  defined by:

$$\begin{cases} I_{rqref} = \frac{L_r \sigma L_s}{V_s R_s M} \left( \dot{P}_{sref} + K_1 e_1 + \frac{V_s M}{L_s L_r \sigma} \left( V_{rq} - L_r \sigma \omega_r I_{rd} - g \frac{M V_s}{L_s} \right) \right) \\ I_{rdref} = \frac{L_r \sigma L_s}{V_s R_s M} \left( \dot{Q}_{sref} + K_2 e_2 + \frac{V_s M}{L_s L_r \sigma} \left( V_{rd} + L_r \sigma \omega_r I_{rq} \right) \right) \end{cases} \quad (36)$$

$I_{rdref}$  and  $I_{rqref}$  will be considered as reference to the following subsystem.

### Step 2: Calculation of rotor voltages:

In this last step, it has been possible to deduce the true control law  $V_{rq}$  and  $V_{rd}$  which makes it possible to reach the design objectives for the global system. The errors of the rotor currents are defined by:

$$\begin{cases} e_3 = I_{rqref} - I_{rq} \\ e_4 = I_{rdref} - I_{rd} \end{cases} \quad (37)$$

The derivative of the errors is given by:

$$\begin{cases} \dot{e}_3 = \dot{I}_{rqref} - \dot{I}_{rq} \\ \dot{e}_4 = \dot{I}_{rdref} - \dot{I}_{rd} \end{cases} \quad (38)$$

$$\begin{cases} \dot{e}_3 = \dot{I}_{rqref} - \frac{1}{L_r \sigma} \left( V_{rq} - R_r I_{rq} - L_r \sigma \omega_r I_{rd} - g \frac{M V_s}{L_s} \right) \\ \dot{e}_4 = \dot{I}_{rdref} - \frac{1}{L_r \sigma} \left( V_{rd} - R_r I_{rd} + L_r \sigma \omega_r I_{rq} \right) \end{cases} \quad (39)$$

The extended LYAPUNOV function becomes as follows:

$$V_2 = \frac{1}{2} e_1^2 + \frac{1}{2} e_2^2 + \frac{1}{2} e_3^2 + \frac{1}{2} e_4^2 \quad (40)$$

The derivative becomes:

$$\dot{V}_2 = e_1 \dot{e}_1 + e_2 \dot{e}_2 + e_3 \dot{e}_3 + e_4 \dot{e}_4 = \dot{V}_1 + e_3 \dot{e}_3 + e_4 \dot{e}_4 \quad (41)$$

In order to ensure the stability of the system according to LYAPUNOV,  $\dot{V}_2$  must be negative. So, we choose it in the following form:

$$\dot{V}_2 = -K_1 e_1^2 - K_2 e_2^2 - K_3 e_3^2 - K_4 e_4^2 \leq 0 \quad (42)$$

Equalizing the two equations, we obtain:

$$\begin{aligned} \dot{V}_2 = \dot{V}_1 + e_3 \left( \dot{I}_{rqref} - \frac{1}{L_r \sigma} \left( V_{rq} - R_r I_{rq} - \omega_r L_r \sigma I_{rd} - g \frac{M V_s}{L_s} \right) \right) + \\ e_4 \left( \dot{I}_{rdref} - \frac{1}{L_r \sigma} \left( V_{rd} - R_r I_{rd} + \omega_r L_r \sigma I_{rq} \right) \right) = \dot{V}_1 - K_3 e_3^2 - K_4 e_4^2 \end{aligned} \quad (43)$$

So, we get:

$$\begin{cases} e_3 \left( \dot{I}_{rqref} - \frac{1}{L_r \sigma} \left( V_{rq} - R_r I_{rq} - \omega_r L_r \sigma I_{rd} - g \frac{M V_s}{L_s} \right) \right) = -K_3 e_3^2 \\ e_4 \left( \dot{I}_{rdref} - \frac{1}{L_r \sigma} \left( V_{rd} - R_r I_{rd} + \omega_r L_r \sigma I_{rq} \right) \right) = -K_4 e_4^2 \end{cases} \quad (44)$$

Which gives the expression global real command  $V_{rd}$  and  $V_{rq}$  defined by:

$$\begin{cases} V_{rd} = L_r \sigma \left( K_4 e_4 + \dot{I}_{rdref} + \frac{1}{L_r \sigma} \left( R_r I_{rd} - \omega_r L_r \sigma I_{rq} \right) \right) \\ V_{rq} = L_r \sigma \left( K_3 e_3 + \dot{I}_{rqref} + \frac{1}{L_r \sigma} \left( R_r I_{rq} + \omega_r L_r \sigma I_{rd} + g \frac{M V_s}{L_s} \right) \right) \end{cases} \quad (45)$$

Hence, the asymptotic stability of the origin.

With:  $k_3, k_4$  are positive constants.

### 4.2.2 GSC control using Backstepping controllers

The powers exchanged between the Grid Side Converter GSC and network are expressed by [14]:

$$\begin{cases} P_f = v_{qs} I_{qf} \\ Q_f = -v_{qs} I_{df} \end{cases} \quad (46)$$

The expression of the filter currents is presented by the following equation:

$$\begin{cases} \dot{I}_{df} = -\frac{V_{df}}{L_f} - \frac{R_f}{L_f} I_{df} + \omega_s I_{qf} \\ \dot{I}_{qf} = -\frac{V_{qf}}{L_f} - \frac{R_f}{L_f} I_{qf} - \omega_s I_{df} + \frac{V_s}{L_f} \end{cases} \quad (47)$$

According to these equations, we notice that the active and reactive powers are linked by the filter currents. So, it is sufficient to control the currents of the filter; the direct component  $I_{qf}$  controls the active power of the filter  $P_f$  and the quadratic component  $I_{df}$  controls the reactive power of the filter  $Q_f$ .

The errors of the filter currents  $e_5$  and  $e_6$  are defined by:

$$\begin{cases} e_5 = I_{dfref} - I_{df} \\ e_6 = I_{qfref} - I_{qf} \end{cases} \quad (48)$$

The derivatives of the errors are given by:

$$\begin{cases} \dot{e}_5 = Id_{fref} - I_{df} \\ \dot{e}_6 = Iq_{fref} - I_{qf} \end{cases} \quad (49)$$

By replacing the filter currents, we obtain the following equation:

$$\begin{cases} \dot{e}_5 = Id_{fref} + \frac{V_{df}}{L_f} + \frac{R_f}{L_f} I_{df} - \omega_s I_{qf} \\ \dot{e}_6 = Iq_{fref} + \frac{V_{qf}}{L_f} + \frac{R_f}{L_f} I_{qf} + \omega_s I_{df} - \frac{V_s}{L_f} \end{cases} \quad (50)$$

We choose the candidate function of " LYAPUNOV " associated with the filter current errors, in the following quadratic form:

$$V_3 = \frac{1}{2} e_5^2 + \frac{1}{2} e_6^2 \quad (51)$$

Its derivative is given by:

$$\dot{V}_3 = e_5 \dot{e}_5 + e_6 \dot{e}_6 \quad (52)$$

$$\dot{V}_3 = e_5 \left( Id_{fref} + \frac{V_{df}}{L_f} + \frac{R_f}{L_f} I_{df} - \omega_s I_{qf} \right) + e_6 \left( Iq_{fref} + \frac{V_{qf}}{L_f} + \frac{R_f}{L_f} I_{qf} + \omega_s I_{df} - \frac{V_s}{L_f} \right) \quad (53)$$

So as to ensure the stability of the subsystem according to LYAPUNOV,  $\dot{V}_3$  must be negative. So, we choose it in the following form:

$$\dot{V}_3 = -K_5 e_5^2 - K_6 e_6^2 \leq 0 \quad (54)$$

With:  $k_5, k_6$  are positive constants.

By doing the equality between the two equations, we get:

$$\begin{aligned} e_5 \left( Id_{fref} + \frac{V_{df}}{L_f} + \frac{R_f}{L_f} I_{df} - \omega_s I_{qf} \right) + e_6 \left( Iq_{fref} + \frac{V_{qf}}{L_f} + \frac{R_f}{L_f} I_{qf} + \omega_s I_{df} - \frac{V_s}{L_f} \right) \\ = -K_5 e_5^2 - K_6 e_6^2 \end{aligned} \quad (55)$$

So:

$$\begin{cases} e_5 \left( Id_{fref} + \frac{V_{df}}{L_f} + \frac{R_f}{L_f} I_{df} - \omega_s I_{qf} \right) = -K_5 e_5^2 \\ e_6 \left( Iq_{fref} + \frac{V_{qf}}{L_f} + \frac{R_f}{L_f} I_{qf} + \omega_s I_{df} - \frac{V_s}{L_f} \right) = -K_6 e_6^2 \end{cases} \quad (56)$$

Which gives the expression of the actual global command  $V_{fd}$  and  $V_{fq}$  defined by:

$$\begin{cases} V_{df} = -L_f \left( K_5 e_5 + Id_{fref} + \frac{R_f}{L_f} I_{df} + \omega_s I_{qf} \right) \\ V_{qf} = -L_f \left( K_6 e_6 + Iq_{fref} + \frac{R_f}{L_f} I_{qf} + \omega_s I_{df} - \frac{V_s}{L_f} \right) \end{cases} \quad (57)$$

## 5 Results and discussion

To gauge the performance of the wind system based on the Doubly Fed Induction Generator, we tested the operation of the wind system by two types of control: the sliding mode technique and the BACKSTEPPING one in order to control the powers generated by the DFIG. To carry out this work, two tests were performed using MATLAB / Simulink:

- Test 1: Tracking and regulation tests for SMC and PI.
- Test 2: The robustness tests regarding the variation parameters.

The results obtained for the various simulation tests, are respectively exposed on the following figures:

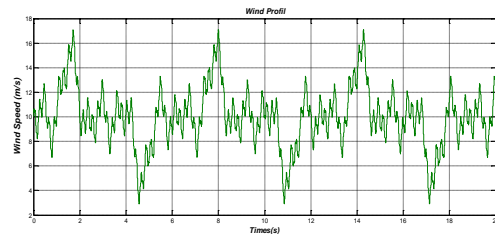
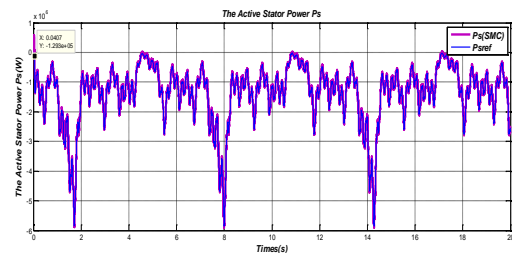


Figure.3: Wind Profile

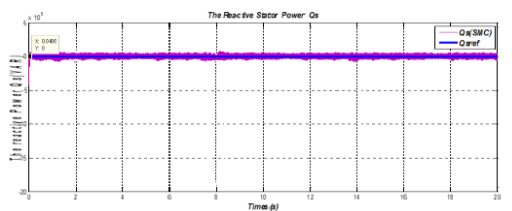
### 5.1 Tracking and Regulation Tests:

In this case, we consider the aerodynamic power according to the MPPT strategy as a reference for the stator active power of the DFIG and zero as a reference of the stator reactive power to guarantee a unit power factor on the stator side to optimize the quality of the energy reverted on the grid.

#### 5.1.1 Sliding Mode Controller results:



(a)



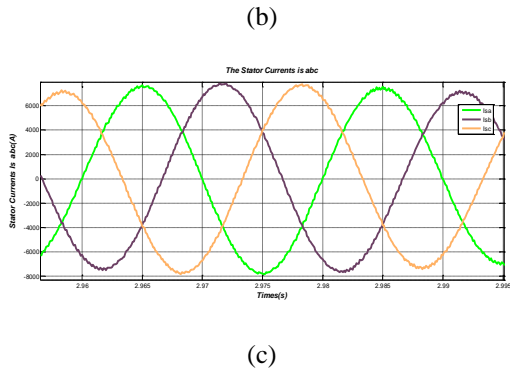


Figure.4: Tracking and regulation Tests using Sliding Mode Controller  
Using the sliding mode technique (figure.4) we note that:  
The references of the powers are well followed by the generator without coupling effect between the two axes and a response time  $T_r = 0.0407s$ .  
The active stator power  $P_s$  (a) is negative means that the Grid receives the energy produced by the DFIG.  
The reactive stator power (b) is null which gives a unit power factor.  
The stator voltages are a sinusoidal form with a fixed frequency 50Hz which implies a clean energy exchanges between the stator and the Grid.  
But the major problem of the sliding mode controller lies in the chattering phenomenon which destabilizes the wind system.

**5.1.2 Backstepping Controller results:**

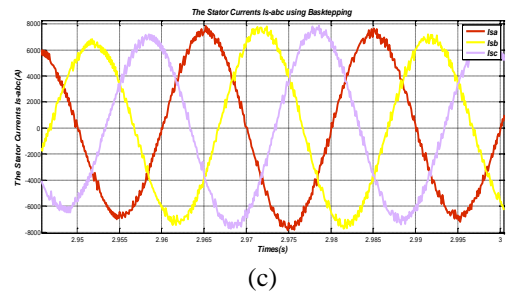
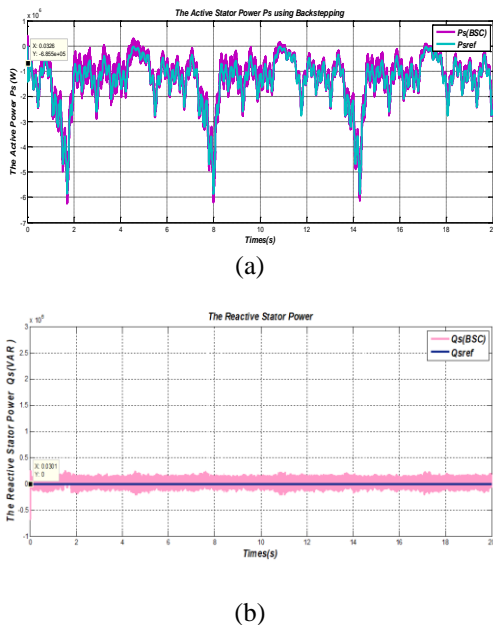


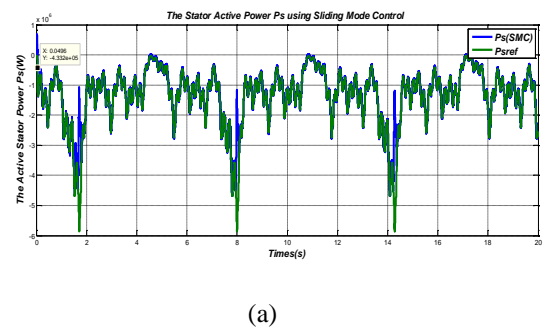
Figure.5: Tracking and regulation Tests using Backstepping Controller  
The BACKSTEPPING control technique (figure.5) gives the following results:  
Good reference tracking by the DFIG generator with a response time obtained  $T_r = 0.03s$  which is less than the response time obtained by the sliding mode technique.

**5.2 Robustness Tests:**

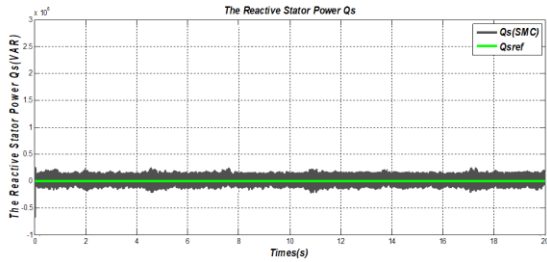
The previous test was done considering the fixed machine parameters, but these parameters can be influenced by several physical phenomena such as the temperature which allows the increase of the resistance values, the saturation of the inductors etc... In addition, the identification of these parameters is expressed in infidelities owing to measuring devices and the adopted methodology. Therefore, it is interesting to compare the performance of both systems regarding this phenomenon. To test the performance of each controller against model uncertainties affecting system stability, we replace the parameters of the system used in the DFIG by the following equation:

$$\{R_{(s,r)} = 0.8R_n, L_{(s,r)} = 1.8L_n$$

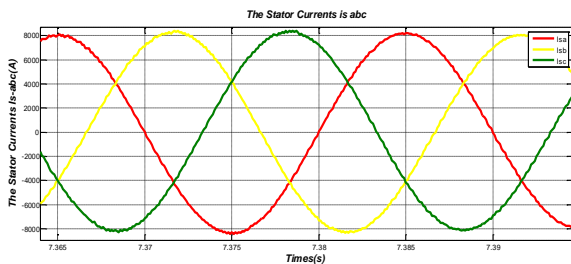
**5.2.1 Sliding Mode Controllers results**







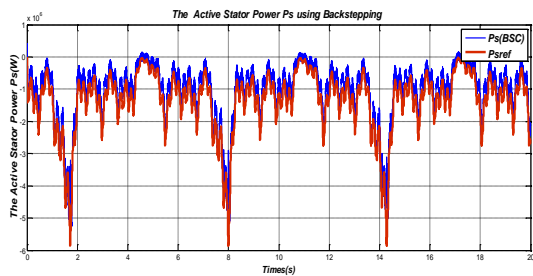
(b)



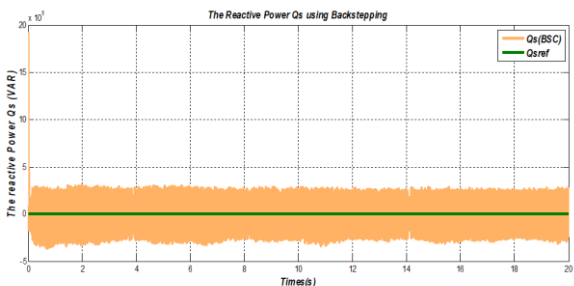
(c)

Figure.6: Robustness Tests using Sliding Mode Controller

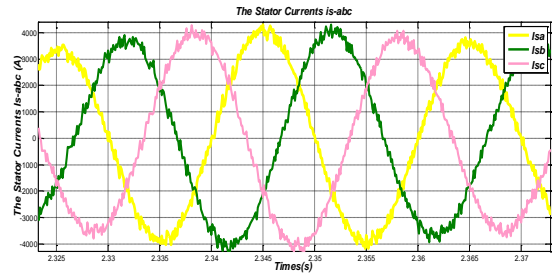
5.2.2 Backstepping Controllers results



(a)



(b)



(c)

Figure.7: Robustness Tests using Backstepping Controller

When we change the parameters of the machine DFIG, we can see a small variation in the response time of the two controllers. On the other hand, this result shows a clear effect in permanent error using the backstepping controller, which implies that the Sliding Mode Controller is more robust than the Backstepping Controller.

6 Conclusion

This work presents a nonlinear power control of doubly-fed induction generator integrated in the Wind System. First, the model of the doubly fed induction generator under the park referential is presented. Secondly, a control strategy using sliding mode and backstepping is shown. The simulation results demonstrate the performance of the controllers. It is clear that the disadvantage of sliding mode is the chattering phenomenon that generates the harmonics and helps to stress the mechanical part, while the problem of the backstepping is not robust against the machine variation parameters. All this leads us to think of other improvements such as moving to a higher order sliding mode to eliminate the chattering phenomenon and the adaptive backstepping control to make the system robust, or to hybridize the two techniques of control.

References:

[1] X. S. Li, et al., "Analysis and Simplification of Three-Dimensional Space Vector PWM for Three-Phase Four-Leg Inverters," IEEE Transactions on Industrial Electronics, vol. 58, pp. 450-464, Feb 2011.

[2] Canudas,D., Commande des moteurs asynchrone, modélisation contrôle vectoriel et DTC ,HERMES/LAVOISIER ,Paris, (2000).

[3] Gille, J. C., Decaulne, P., & Pélegrin, M. "Systèmes asservis non linéaires" ,5,Dunod. (1975).

[4] LOUCIF, M., "Synthèse de lois de commande non-linéaires pour le contrôle d'une machine asynchrone à double alimentation dédiée à un système aérogénérateur",Phd.Thesis, Université



- Aboubakr Belkaïd, Faculté de TECHNOLOGIE-Tlemcen-, (2016).
- [5] Buhler,H., “Réglage par mode de glissement. ”, Première Edition. éd., Lausanne, Suisse: Presses Polytechniques et Universitaires Romandes.( 1986),
- [6] BEKAKRA,Y., “Contribution à l’Etude et à la Commande Robuste d’un Aérogénérateur Asynchrone à Double Alimentation.”, Phd.Thesis, Université Mohamed Khider, Biskra., (2014).
- [7] Ihedrane ,Y., EL Bekkali, C. , Bossoufi, B. , “Power Control of DFIG-generators for Wind Turbines Variable-speed. ”, International Journal of Power Electronics and Drive Systems (IJPEDS) ,8(1):444-453, (2017).
- [8] Bossoufi, B., Ionita, S., Constantinescu, L., Alami Arroussi , H., El Ghamrasni, M. , & Ihedrane, Y., “Managing voltage drops: a variable speed wind turbine connected to the grid”, International Journal of Automation and Control , 11(1):15-34 ,(2017)
- [9] Bossoufi, B., Karim ,M., Lagrioui ,A., Taoussi ,M.,Derouich ,A., “Observer backstepping control of DFIG-Generators for wind turbines variable-speed: FPGA-based implementation.” Renewable Energy (ELSIVER), 81: 903-917,( 2015)
- [10] Amimeur,H.,Aouzellag,D.,Abdessemed,R.,Ghedamsi, K.,“Sliding mode control of a dual-stator induction generator for wind energy conversion systems. ”, International Journal of Electrical Power & Energy Systems, 42(1):60-70, (2012)
- [11] Ihedrane ,Y., EL Bekkali, C. , Bossoufi, B. , “Direct and indirect field oriented control of DFIG-generators for wind turbines variable-speed.”, 14th International Multi-Conference on Systems, Signals & Devices (SSD), Marrakech -Morocco-, 28-31 (March 2017).
- [12] Aouzellag,D., Ghedamsi, K., Berkouk,E.M., “ Network power flux control of a wind generator.”, Renewable Energy, 34(3): 615-622,(2009).
- [13] Bekakra,Y., Ben Attous, D., “DFIG sliding mode control fed by back-to-back PWM converter with DC-link voltage control for variable speed wind turbine,” Frontiers in Energy, 8 : 345–354 , (2014).
- [14] MACHMOUM, M. et POITIERS,F.,“Sliding mode control of a variable speed wind energy conversion system with DFIG.”,Ecologic vehicles; renewable energies, MONACO,(March 2009).
- [15] TAMAARAT ,A., “Modélisation et commande d’un système de conversion d’énergie éolienne à base d’une MADA.”, Phd.Thesis, Université Mohamed Khider,Biskra, (2015).
- [16] Bregeault, V., “Quelques contributions à la théorie de la commande par modes glissants.”, Phd.Thesis, Ecole Centrale de Nantes (ECN). (2010).
- [17] Slotine, J. J., and W. Li. ,“Applied Nonlinear Control, Prentice-Hall, Englewood Cliffs, NJ, 1991.”, 461,Google Scholar (1998).
- [18] Hashimoto, H., Yamamoto, H., Yanagisawa, S., & Harashima, F. , “Brushless servo motor control using variable structure approach”,IEEE Transactions on industry applications, 24(1), 160-170, (1988).
- [19] HAMDI ,N., “Amélioration des performances des aérogénérateurs. ”, Phd.Thesis, Université Constantine I ,(2013).
- [20] Taoussi, M., Karim, M., Bossoufi, B., Hammoumi, D., Lagrioui, A., & Derouich, A. (2016). Speed variable adaptive backstepping control of the doubly-fed induction machine drive. International Journal of Automation and Control, 10(1), 12-33.
- [21] Bossoufi, B. A. D. R. E., Karim, M. O. H. A. M. M. E. D., Ionita, S. I. L. V. I. U., & Lagrioui, A. H. M. E. D. (2011). The optimal direct torque control of a PMSM drive: FPGA-based implementation with MATLAB & Simulink simulation. Journal of Theoretical and Applied Information Technology JATIT, 28(2), 63-72
- [22] Jerbi,L., Krichen,L., Ouali,A., “A fuzzy logic supervisor for active and reactive power control of a variable speed wind energy conversion system associated to a flywheel storage system, ”, Electric power systems research, Elsevier , 79(6): 919-925, (2009).
- [23] El Ouanjli, N., Derouich, A.,El Ghzizal, A.,El Mourabet ,Y., Bossoufi,B., Taoussi,M., "Contribution to the performance improvement of Doubly Fed Induction Machine functioning in motor mode by the DTC control", International Journal Power Electronics and Drive System , 8 (3): 1117-1127,(2017).
- [24] N. El Ouanjli, et al., “High Performance Direct Torque Control of Doubly Fed using Fuzzy Logic,” Gazi University Journal of Science, vol.31, No. 2, pp. 532-542, 2018.